Weierstraß-Institut

für Angewandte Analysis und Stochastik

Leibniz-Institut im Forschungsverbund Berlin e. V.

Preprint ISSN 2198-5855

Multi-stability and polariton soliton formation in microcavity polaritonic waveguides

Gabriela Slavcheva[1], Andrey V. Gorbach[1], Alexander Pimenov[2],

Andrei G. Vladimirov[2], Dmitry V. Skryabin[1]

submitted: March 5, 2015

[1] Department of Physics
University of Bath
Bath
BA2 7AY
United Kingdom
E-Mail: g.slavcheva@bath.ac.uk

[2] Weierstrass Institute
Mohrenstr. 39
10117 Berlin
Germany
E-Mail: alexander.pimenov@wias-berlin.de
andrei.vladimirov@wias-berlin.de

No. 2090

Berlin 2015

2010 *Physics and Astronomy Classification Scheme.* 05.45.-a, 42.65.Pc, 42.65.Tg.

Key words and phrases. Polaritons, solitons, microcavities, multi-stability, tilted waveguides.

Funding through Leverhulme Trust Research Project Grant RPG-2012-481 is gratefully acknowledged. A. P. and A. G. V. acknowledge the support of SFB 787 of the DFG, project B5.

Edited by
Weierstraß-Institut für Angewandte Analysis und Stochastik (WIAS)
Leibniz-Institut im Forschungsverbund Berlin e. V.
Mohrenstraße 39
10117 Berlin
Germany

Fax: +49 30 20372-303
E-Mail: preprint@wias-berlin.de
World Wide Web: http://www.wias-berlin.de/

Abstract

Nonlinear polaritons in microcavity waveguides are demonstrated to exhibit multi-stable behaviour and rich dynamics, including filamentation and soliton formation. We find that the multi-stability originates from co-existense of different transverse modes of the polaritonic waveguide. Modulational stability and conditions for multi-mode polariton solitons are studied. Soliton propagation in tilted, relative to the pump momentum, waveguides is demonstrated and a critical tilt angle for the soliton propagation is found.

Strong exciton-photon coupling in semiconductor microcavities leads to formation of half-light half-matter quasiparticles (polaritons) [1]. Owing to their excitonic component polaritons exhibit very strong and fast nonlinear optical response and weaker diffraction. These properties make microcavity polaritons an attractive platform for developing prototypes of opto-eletronic devices for processing of information. Effects and devices such as low threshold optical bistability [2], optical switches [3], optical transistors [4], diodes [5] and Mach-Zehnder interferometer [6] have been demonstrated with microcavity polaritons. Recently, dark [7, 8] and bright microcavity polariton solitons [9, 10, 11] have been reported theoretically and experimentally. Solitons in planar microcavities operating in non-polaritonic regimes have been previously studied in the context of optical information buffering and memory devices [12, 13]. Polaritonic regimes of operation can be useful in optimizing these devices for lower power consumption and more compact dimensions. Large-aperture planar devices, can not be used to predictably bend trajectory of a polaritonic pulse or to make polaritonic couplers, X and Y junctions and interferometers. Lateral waveguide confinement can effectively boost polariton-polariton interaction and reduce the number of polaritons required for nonlinear processes, allowing observation of quantum effects such as squeezing, phase transitions, polaritonic blockade and others [14]. Previous studies of 2D microcavity polariton solitons have shown that the diffraction in a transverse to the soliton velocity direction is balanced only in a very narrow range of parameters [15] and microcavity mirror patterning has been suggested for guided solitons [9]. An alternative, well studied for soliton applications geometry, is total internal-reflection based semiconductor waveguides with quantum wells embedded inside the substrate (see, e.g., [16]). Transition into the strong coupling regime in these structures has been reported only recently [17]. Despite being more difficult to fabricate, microcavity waveguides have an advantage of providing significant group velocity reduction and employing well established resonant or nonresonant pumping schemes for loss compensation.

Considering ongoing experimental research into microcavity polariton waveguides it becomes important to extend the theoretical understanding of the nonlinear effects, such as bistability, parametric generation and solitons using experimentally realistic geometries and conditions. In this Letter, we use an established dimensionless mean-field model for photonic and excitonic components of microcavity polaritons, see, e.g. [7, 9, 10], whereby an effective transverse con-

finement potential is introduced:

$$\partial_t E - i\left(\partial_x^2 + \partial_y^2\right) E + \left[\gamma_c - i\delta_c - i\Delta - iU(y)\right] E = i\Omega_R(y)\Psi + E_p e^{i\kappa x} \ , \quad (1)$$

$$\partial_t \Psi + \left(\gamma_e - i\delta_e - i\Delta\right)\Psi + i\left|\Psi\right|^2 \Psi = i\Omega_R(y) E \ . \quad (2)$$

Here, E and Ψ are the averages of the photon and exciton creation or annihilation operators, the normalization is such that $(\omega_R/g)|E|^2$ and $(\omega_R/g)|\Psi|^2$ are the photon and exciton numbers per unit area, g is the strength of exciton-exciton interaction [10], ω_R is the Rabi frequency in a planar homogeneous cavity, time is measured in the units of $T = 1/\omega_R$. The waveguide geometry is schematically shown in Fig. 1(a). The unit length, $L = \sqrt{\hbar/(2m_c\omega_R)}$ [7, 9], is determined by the effective cavity photon mass m_c. The waveguide confinement in the cavity plane (along y-axis) is described by an effective potential $U(y)$ in the photonic component and a spatially confined normalized Rabi frequency $\Omega_R(y)$:

$$U(y) = U_{bg}\left[1 - e^{-(2y/w)^8}\right] \ , \ \Omega_R(y) = e^{-(2y/w)^8} \ , \quad (3)$$

where w is the dimensionless waveguide width.

We assume that the CW pump with normalized amplitude E_p is linearly polarized along y-axis, so that it mainly couples to quasi-TE waveguide modes, thus justifying the use of a scalar model. The pump is inclined along x-axis, so that κ is the momentum component along the waveguide, the corresponding angle θ is such that $\sin\theta = \kappa\lambda_p/(2\pi L)$, λ_p is the pump wavelength. The parameters δ_c, δ_e and Δ are dimensionless detunings of the cavity resonant frequency, excitonic resonance, and pump frequency from a reference frequency $\hbar\omega_0 = 1.55$eV ($\lambda_0 = 800$nm), respectively. Cavity and exciton damping constants are set equal: $\gamma_c = \gamma_e = \gamma$.

Particular values for the parameters ω_R, L and U_{bg} are chosen to fit the free polariton dispersion in a realistic waveguide geometry, inferred from finite-element Maxwell solver (Comsol). As an example, we consider a 3μm-wide waveguide with a 400nm-thick cavity ($\epsilon_c = 9$) and distributed Bragg reflector (DBR) mirrors, each containing 25 periods of alternating low- and high-index layers ($\epsilon_l = 9$, $\epsilon_h = 12.25$) of thickness $L_l = \lambda_0/(4\sqrt{\epsilon_l})$ and $L_h = \lambda_0/(4\sqrt{\epsilon_h})$, respectively. The empty cavity resonance for the fundamental mode is found to be at $\hbar\omega_c \approx 1.551$eV. The quantum well is modelled by a 15nm-thick layer with linear permittivity:

$$\epsilon_{qw} = \epsilon_c + \frac{H\omega_e^2}{\omega^2 - \omega_e^2 - i2\Gamma_e\omega_e} \ , \quad (4)$$

where $\hbar\omega_e = 1.5505$eV, with ω_e - the exciton resonance transition frequency, $H = 0.015$ is the normalised oscillator strength and $\hbar\Gamma_e$ is the exciton linewidth due to dephasing, assumed to be of the order of $0.1meV$ [10].

Photon-exciton coupling causes Rabi splitting of each of the modes into lower- and upper-polaritonic branches. Numerically computed energy dispersions for the first three lower polariton modes ($0L$, $1L$ and $2L$) and for the upper branch (OU) fundamental mode polaritons are shown in Fig. 1(b). For the chosen H the Rabi splitting in the fundamental mode is found to be $2\hbar\omega_R \approx 11$meV at $\kappa = 0$, which is comparable to the one in planar cavities [10]. This gives the scaling of time $T \approx 0.12$ps, and dimensionless cavity and exciton detunings: $\delta_c = -0.191$ and

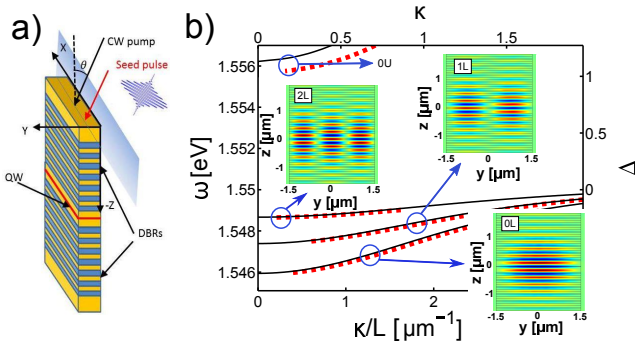

Figure 1: Microcavity polaritonic waveguide: a) scheme of the geometry and excitation; b) Dispersion of free polaritons in the 3μm-wide waveguide: dashed lines correspond to data obtained from Comsol, solid lines - from model in Eqs. (1, 2). Insets show profiles of the dominant electric field component (E_y) of the first three quasi-TE modes.

$\delta_e = -0.1$, respectively. The free polariton dispersion within our model in Eqs.(1,2) fits well the above computed dispersion by fixing $L = 0.53\mu$m and $U_{bg} = -1$ (solid curves in Fig. 1(b)).

Similar to a planar cavity, the lower polariton effective mass changes its sign for transverse momenta $\kappa/L \gtrsim 1.2\mu m^{-1}$. Hence, we expect to observe excitation of bright solitons with large enough transverse (in-plane) momenta [10]. We choose $\kappa/L = 2.69\mu\mathrm{m}^{-1}$ beyond the inflection points in all branches, yielding a pump incidence angle, $\theta \approx 20^\circ$ at $\lambda_p = 800$nm ($\Delta = 0$).

For a spatially homogeneous monochromatic pump, the stationary modes of Eqs. (1,2) are found using the ansatz $\{E, \Psi\} = \{A\,(y)\, e^{i\kappa x}, B\,(y)\, e^{i\kappa x}\}$. The resulting equations for A and B are solved numerically. In the zero pump and zero loss limit of Eqs. (1,2), $E_p = \gamma = 0$ we find that the nonlinear waveguide modes are continuously parameterized by the detuning Δ, see dashed curves in Fig. 2(a), and their number is increasing with Δ. For $E_p = const \neq 0$, each mode with even symmetry ($OL, 2L, 4L, \dots$) exhibits a nonlinear resonance, see solid curves in Fig. 2(a). For pump frequencies above one or several branches of polaritonic dispersion, microcavity waveguides can show either bistable or, respectively, multi-stable response. This is in contrast to planar homogeneous cavities, which are only bistable.

The waveguide modes, however, can be modulationally unstable, similar to the homogeneous solution in a planar cavity. To analyze this we add small perturbations to the modal profiles: $E = [A(y) + \epsilon_f(y)e^{iqx-i\delta t+\lambda t} + \epsilon_b^*(y)e^{-iqx+i\delta t+\lambda t}]e^{i\kappa x}$, $\Psi = [B(y) + p_f(y)e^{iqx-i\delta t+\lambda t} + p_b^*(y)e^{-iqx+i\delta t+\lambda t}]e^{i\kappa x}$ with q, δ, λ all real. The resulting eigenvalue problem:

$$(\delta + i\lambda)\vec{x} = \begin{bmatrix} -\mathcal{L}_f & 0 & -\Omega_R & 0 \\ 0 & \mathcal{L}_b^* & 0 & \Omega_R \\ -\Omega_R & 0 & -\mathcal{P} & B^2 \\ 0 & \Omega_R & -(B^*)^2 & \mathcal{P}^* \end{bmatrix} \vec{x}\,, \tag{5}$$

$$\mathcal{L}_{f,b} = \partial_y^2 - (\kappa \pm q)^2 + \delta_c + \Delta + U + i\gamma_c,$$

$$\mathcal{P} = \delta_e + \Delta - 2|B|^2 + i\gamma_e\,,\ \vec{x} = [\epsilon_f, \epsilon_b, p_f, p_b]^T\,,$$

is solved numerically.

In Figs. 2(b) and (c) stable, unstable (with $\lambda(q = 0) > 0$) and modulationally unstable ($\lambda > 0$

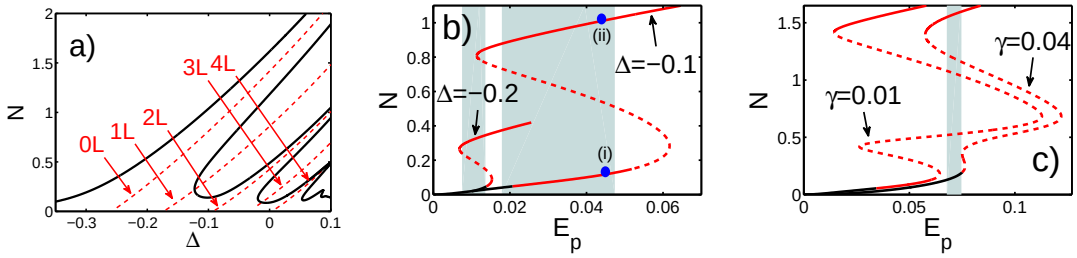

Figure 2: Stationary nonlinear modes (Ψ-norm $N = \int |\Psi|^2 dy$): (a) as function of the detuning Δ, $E_p = 0.005$, $\gamma = 0.01$. Dashed curves indicate families of nonlinear mode solutions $0L$-$4L$ in the limit $E_p = \gamma = 0$; (b) and (c) as functions of the pump amplitude E_p, $\Delta = -0.2$ and $\Delta = -0.1$, $\gamma = 0.01$ in (b), $\Delta = 0$, $\gamma = 0.01$ and $\gamma = 0.04$ in (c). Solid black, dashed red/grey and solid red/grey curves correspond to stable, unstable and modulationally unstable branches, respectively. Shaded areas in (b) and (c) indicate domains of existence of soliton solutions.

only for some $q \neq 0$) branches are plotted as functions of the pump amplitude E_p with solid black, dashed red/grey and solid red/grey curves, respectively, for different values of Δ and γ. For a pump frequency just above the lowest ($0L$) linear mode branch, $\Delta = -0.2$ cf. Fig. 2(a), the stationary waveguide mode is bistable within a certain range of E_p, see Fig. 2(b), where the lowest norm solution is stable, while the highest norm one is modulationally unstable. Similar behaviour is observed in planar cavities, where the co-existence of stable low-amplitude and modulationally unstable high-amplitude stationary modes is accompained by the presence of bright solitons [9, 10].

We numerically found localized soliton solutions of Eqs. (1,2) of the form $\{E, \Psi\} = \{A_s(x - vt, y), B_s(x - vt, y)\}e^{i\kappa x}$, discretizing spatial coordinates and using Newton-Raphson iterations. Here the soliton velocity,v, is computed simultaneously with the soliton field profiles, A_s and B_s. For $\Delta = -0.2$ solitons exist within almost the entire domain of bistability of stationary modes, as shown by the shaded region in Fig. 2(b).

Increasing the pump frequency, the lowest norm stationary mode develops instabilities for E_p close to the turning point. The instability domain gradually expands with increasing pump frequency. For $\Delta = -0.1$, the mode is unstable within a large part of the entire bistability domain, see Fig. 2(b). In Fig. 3(a) the small perturbation gain λ is plotted as function of the perturbation wave vector, q, for the mode at $E_p = 0.045$ [see marker (i) in Fig. 2(b)]. We found that the mode is modulationally unstable with respect to several perturbations, each having a different transverse profile, see insets in Fig. 3(a). The observed instabilities can be attributed to the co-existence of multiple transverse modes in the waveguide potential. By contrast, the modulation instability of stationary modes from the highest norm branch is due to the perturbation with a similar transverse shape as the mode itself (Fig. 3(b)). To verify the above linear stability analysis we solved Eqs.(1,2) in the time domain perturbing solutions (i) and (ii). The evolved perturbed solutions exhibit filamentation and localised soliton-like features (Fig. 3(a,b):right panels).

For $\Delta = -0.1$ soliton solutions exist within a wide range of E_p (see corresponding shaded area of the bistability domain in Fig. 2(b)). However, having the homogeneous stationary mode from the lowest norm branch as their background, solitons share their stability properties with this mode. As a result, there is only a narrow window of E_p, where stable solitons can be excited.

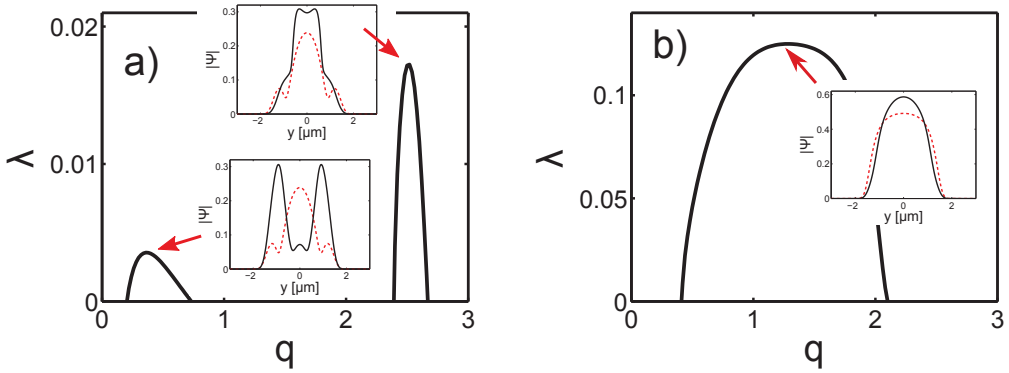

Figure 3: Perturbation growth rate of modulationally unstable modes for $\Delta = -0.1$, $E_p = 0.045$, $\gamma = 0.01$: lower branch (a) and upper branch (b), corresponding solutions are indicated as (i) and (ii) in Fig. 2(b). Insets show profiles (scaled) of unstable perturbations corresponding to local maxima of growth rate. Mode profiles are shown with dashed curves in insets. Right panels: modulation instability time evolution - filamentation (a) and localisation (b).

As the pump frequency crosses the even higher-order polaritonic branch $(2L)$, additional branches of stationary mode solutions emerge, see Figs. 2(a) and (c). The instabilities of the lowest norm branch persist, affecting the existence and stability of solitons. For $\Delta = 0$ and $\gamma = 0.01$ we could not find any stable soliton solutions, and all stationary modes are unstable within almost the entire domain of multi-stability, see Fig. 2(c). Increasing the damping γ, one can stabilize the lowest branch of stationary modes, cf. plots for $\gamma = 0.01$ and $\gamma = 0.04$ in Fig. 2(c). For this higher value of γ we found stable soliton solutions (see shaded area in Fig. 2(c)).

To investigate dynamical formation of solitons within the range of bistability of stationary modes, we initialize the system with the stable mode from the lowest branch. The soliton is triggered by the writing pulse [10], which has duration of 2ps, intensity FWHM of 3μm (Gaussian beam) and the same momentum as the pump. An example of a soliton is shown in Fig. 4 for $\Delta = 0$ and $\gamma = 0.04$. The soliton is sitting on the lowest branch of stationary modes and extends to the highest branch in its core. The soliton pulse is squeezed along the waveguide and its temporal width of $T_p = 0.727\mathrm{ps}$ is nearly a half of that in a planar microcavity ($\sim 1.25\mathrm{ps}$ [10]).

We found that solitons can be excited in waveguides tilted with respect to the pump momentum. Numerically exact soliton solutions, found with Newton-Raphson interations, as functions of the waveguide tilt angle α are plotted in Fig. 5. For fixed parameters of the pump, solitons persist within a finite interval of α, and the tilt can be as high as $\sim 10^\circ$. Further detailed studies of soliton properties and dynamics in polaritonic waveguides will be reported elsewhere.

In summary, we investigated nonlinear polariton dynamics in microcavity waveguides within the modified mean-field model. Parameters of the introduced effective potentials are chosen to fit the free polaritons dispersion in a realistic waveguide geometry. We found that stationary excitations in polaritonic waveguides exhibit multi-stable behaviour upon variation of pump parameters. This is directly related to the existence of different transverse waveguide modes. Modulation instability of stationary modes and soliton formation in straight and tilted waveguides is discussed. Our results lay the foundations for further investigation of basic building blocks of future polaritonic integrated circuits, such as $X-$ and $Y-$splitters, couplers, routers, based on soliton logic.

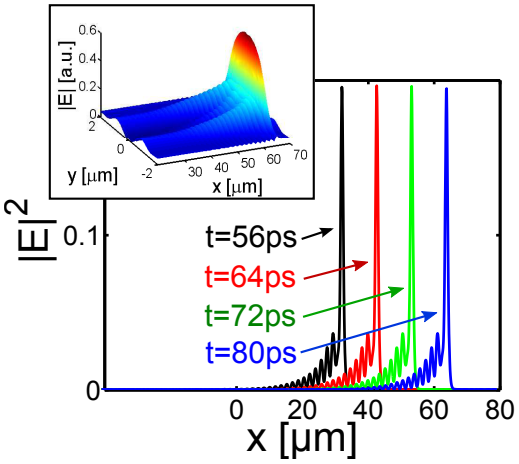

Figure 4: Dynamical soliton formation for $E_p = 0.075$, $\Delta = 0$, and $\gamma = 0.04$, the writing beam is applied at $t = 0$ps: insert - field snapshot at $t = 80$ps; field cross-sections throught the middle of the waveguide ($y = 0$) at different time instants.

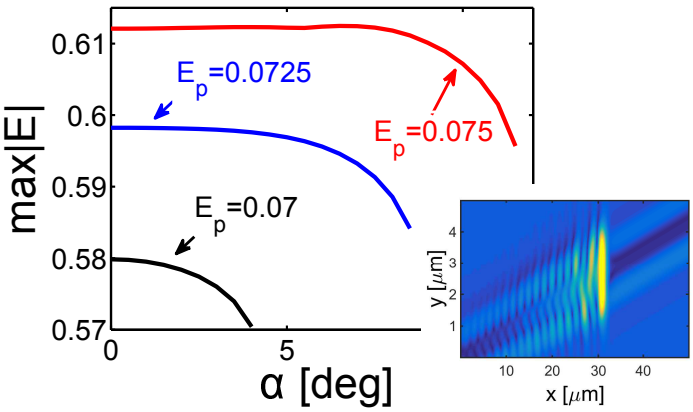

Figure 5: Soliton branches as functions of the waveguide tilt angle α for different amplitudes of the pump and $\Delta = 0$, $\gamma = 0.04$.

References

[1] A. Kavokin, J. Baumberg, G. Malpuech, and F. Laussy, *Microcavities* (Oxford University Press, Oxford, 2007).

[2] A. Baas, J. Karr, H. Eleuch, and E. Giacobino, Öptical bistability in semiconductor microcavities", Phys. Rev. A **69**, 023809 (2004).

[3] A. Amo, T. C. H. Liew, C. Adrados, R. Houdré, E. Giacobino, A. V. Kavokin, and A. Bramati, Ëxciton-polariton spin switches", Nat. Photonics **4**, 361 (2010).

[4] T. Gao, P. S. Eldridge, T. C. H. Liew, S. I. Tsintzos, G. Stavrinidis, G. Deligeorgis, Z. Hatzopoulos, and P. G. Savvidis,"Polariton condensate transistor switch", Phys. Rev. B **85**, 235102 (2012).

[5] H. S. Nguyen, D. Vishnevsky, C. Sturm, D. Tanese, D. Solnyshkov, E. Galopin, A. Lemaître, I. Sagnes, A. Amo, G. Malpuech, and J. Bloch,"Realization of a double-barrier resonant tunneling diode for cavity polaritons", Phys. Rev. Lett. **110**, 236601 (2013).

[6] C. Sturm, D. Tanese, H.S. Nguyen, H. Flayac, E. Galopin, A. Lemaître, I. Sagnes, D. Solnyshkov, A. Amo, G. Malpuech, and J. Bloch, Äll-optical phase modulation in a cavity-polariton Mach-Zehnder interferometer", Nat. Communications **5**, 3278 (2014).

[7] A. V. Yulin, O. A. Egorov, F. Lederer, and D. V. Skryabin, "Dark polariton solitons in semiconductor microcavities,"Phys. Rev. A, **78**, 061801(R) (2008).

[8] A. Amo, T. C. H. Liew, C. Adrados, R. Houdré, E. Giacobino, A. V. Kavokin, and A. Bramati,"Polariton superfluids reveal quantum hydrodynamic solitons,SScience **332**,11167 (2011)

[9] O. A. Egorov, D.V. Skryabin, A.V. Yulin, and F. Lederer, "Bright Cavity Polariton Soliton,"Phys. Rev. Lett. **102**, 153904 (2009).

[10] M. Sich, D. N. Krizhanovskii, M. S. Skolnick, A. V. Gorbach, R. Hartley, D. V. Skryabin, E. A. Cerda-Méndez, K. Biermann, R. Hey, and P. V. Santos, Öbservation of bright polariton solitons in a semiconductor cavity,"Nature Photonics, **6**, 50 (2012).

[11] M. Sich, F. Fras, J. K. Chana, M. S. Skolnick, and D. N. Krizhanovskii, Ëffects of spin-dependent interactions on polarization of bright polariton solitons,"Phys. Rev. Lett. **112**, 046403 (2014)

[12] S. Barland, J. R. Tredicce, M. Brambilla, L. A. Lugiato, S. Balle, M. Giudici, T. Maggipinto, L. Spinelli, G. Tissoni, T. Knödl, M. Miller, and R. Jäger, "Cavity solitons as pixels in semiconductor microcavities", Nature **419**, 699 (2002).

[13] F. Pedaci, S. Barland, E. Caboche, P. Genevet, M. Giudici, J. R. Tredicce, T. Ackemann, A. J. Scroggie, W. J. Firth, G.-L. Oppo, G. Tissoni, and R. Jäger, Äll-optical delay line using semiconductor cavity solitons", Appl. Phys. Lett. **92**, 011101 (2008).

[14] I. Carusotto, and C. Ciuti, "Quantum fluids of light"Rev. Mod. Phys. **85**, 299 (2013).

[15] O. A. Egorov, D.V. Skryabin, A.V. Yulin, and F. Lederer, "Two-dimensional Localization of Exciton Polaritons in Microcavities,"Phys. Rev. Lett. **105**, 073903 (2010).

[16] N. Bêlanger, A. Villeneuve, and J. S. Aitchison, SSolitonlike pulses in self-defocusing AlGaAs waveguides",*J. Opt. Soc. Am. B* **14,** 3003 (1997).

[17] P. M. Walker, L. Tinkler, M. Durska, D. M. Whittaker, I. J. Luxmoore, B. Royall, D. N. Krizhanovskii, M. S. Skolnick, I. Farrer, and D. A. Ritchie, Ëxciton polaritons in semiconductor waveguides", Appl. Phys. Lett. **102**, 012109 (2013).